Development 138, 291-302 (2011) doi:10.1242/dev.055038

The Cdc14B phosphatase contributes to ciliogenesis in zebrafish

Aurélie Clément[1], Lilianna Solnica-Krezel[2,3] and Kathleen L. Gould[1,*]

SUMMARY

Progression through the cell cycle relies on oscillation of cyclin-dependent kinase (Cdk) activity. One mechanism for downregulating Cdk signaling is to activate opposing phosphatases. The Cdc14 family of phosphatases counteracts Cdk1 phosphorylation in diverse organisms to allow proper exit from mitosis and cytokinesis. However, the role of the vertebrate CDC14 phosphatases, CDC14A and CDC14B, in re-setting the cell for interphase remains unclear. To understand Cdc14 function in vertebrates, we cloned the zebrafish *cdc14b* gene and used antisense morpholino oligonucleotides and an insertional mutation to inhibit its function during early development. Loss of Cdc14B function led to an array of phenotypes, including hydrocephaly, curved body, kidney cysts and left-right asymmetry defects, reminiscent of zebrafish mutants with defective cilia. Indeed, we report that motile and primary cilia were shorter in *cdc14b*-deficient embryos. We also demonstrate that Cdc14B function in ciliogenesis requires its phosphatase activity and can be dissociated from its function in cell cycle control. Finally, we propose that Cdc14B plays a role in the regulation of cilia length in a pathway independent of fibroblast growth factor (FGF). This first study of a loss of function of a Cdc14 family member in a vertebrate organism reveals a new role for Cdc14B in ciliogenesis and consequently in a number of developmental processes.

KEY WORDS: Cell cycle, Ciliogenesis, Left-right asymmetry, Zebrafish

INTRODUCTION

Regulation of the cell cycle during embryonic development is crucial to the morphogenesis of tissues and organs of proper shape and size. Key players in this tight regulation are the Cyclin-dependent kinases (Cdks), the oscillating activity of which mediates an orderly progression through the cell cycle (Morgan, 1997). Cdc14 phosphatases reverse Cdk1-dependent phosphorylation events in diverse organisms and therefore contribute to proper mitotic exit and cytokinesis. Like many mitotic regulators, Cdc14 phosphatases localize dynamically through the cell cycle to diverse cellular structures, where they presumably act on various substrates (Trinkle-Mulcahy and Lamond, 2006).

Cdc14 was first discovered in *Saccharomyces cerevisiae*, where it is essential for mitotic exit (Stegmeier and Amon, 2004). Cdc14 has been conserved throughout evolution and performs orthologous functions in other organisms (Clifford et al., 2008; Stegmeier and Amon, 2004). However, Cdc14 enzymes are not essential for cell division in *Schizosaccharomyces pombe* (Cueille et al., 2001; Trautmann et al., 2001) or *Caenorhabditis elegans* (Saito et al., 2004), indicating that redundant phosphatases must be involved in mitotic exit in these organisms.

In vertebrates, Cdc14 is encoded by at least two genes, *CDC14A* and *CDC14B*. Studies in cell culture and *Xenopus laevis* and mouse oocytes have implicated CDC14A in mitosis, cytokinesis (Bembenek and Yu, 2001; Kaiser et al., 2004; Kaiser et al., 2002; Krasinska et al., 2007; Mailand et al., 2002), meiosis (Schindler and Schultz, 2009b) and DNA repair (Mocciaro et al., 2010), whereas CDC14B is reported to act in G1-phase length regulation (Rodier et al., 2008), centriole duplication (Wu et al., 2008), spindle stability (Cho et al., 2005), meiosis (Schindler and Schultz, 2009a), DNA damage response or repair (Bassermann et al., 2008; Mocciaro et al., 2010) and activation of the zygotic genome (Buffone et al., 2009). Interestingly, CDC14B is dispensable for cell proliferation in human cell culture (Berdougo et al., 2008). Taken together, our knowledge about CDC14 phosphatase function in vertebrates, particularly at the organismal level, remains limited.

To investigate CDC14 function during vertebrate development, we used zebrafish. The zebrafish genome contains three *cdc14* genes that we found to be ubiquitously expressed throughout embryogenesis. Two of the genes encode Cdc14A paralogs, whereas the third encodes Cdc14B. Using an antisense morpholino oligonucleotide (MO) approach and an insertional mutation in the *cdc14b* locus to inhibit Cdc14B function during early development, we observed that *cdc14b*-deficient embryos developed through embryonic and early larval stages, but manifested a variety of abnormalities, including hydrocephaly, curved body, kidney cysts and defects in left-right (LR) asymmetry, which were reminiscent of phenotypes in zebrafish mutants with defective cilia (Bisgrove and Yost, 2006; Kramer-Zucker et al., 2005). Indeed, we found that Cdc14B is necessary for proper cilia formation in the Kupffer's vesicle (KV), the kidney duct and the sensory patches of the inner ear. The phosphatase activity of Cdc14B is required for its role in ciliogenesis as it is for its role in cell division control; these functions of Cdc14B can be dissociated from one another. Our study has uncovered a new role for Cdc14 phosphatases in vertebrates and suggests that the process of ciliogenesis and consequently a number of developmental processes are exquisitely sensitive to Cdc14B function.

[1]Howard Hughes Medical Institute and Department of Cell and Developmental Biology, Vanderbilt University School of Medicine, Nashville, TN 37232, USA.
[2]Department of Biological Sciences, Department of Cell and Developmental Biology, Department of Pediatrics, Vanderbilt University, Nashville, TN 37235, USA.
[3]Department of Developmental Biology, Washington University School of Medicine, St Louis, MO 63110, USA.

*Author for correspondence (kathy.gould@vanderbilt.edu)

Accepted 8 November 2010

MATERIALS AND METHODS

Zebrafish maintenance and staging

Wild-type (WT) AB*, *cdc14b*$^{vu426/vu426}$, *tp53*$^{zdf1/zdf1}$ (Berghmans et al., 2005), *Tg[cmlc2:GFP]*, *Tg[sox17:GFP]* (Sakaguchi et al., 2006) and *ace*$^{x15/+}$ adult zebrafish, *Danio rerio*, were maintained as described previously (Solnica-Krezel et al., 1996). Embryos were staged according to morphology (Kimmel et al., 1995).

cdc14 gene cloning and sequence analysis

cdc14 cDNAs were amplified from a cDNA library obtained from 24 hours post fertilization (hpf) embryos (see Table S1 in the supplementary material), except for *cdc14b_tv2*, which was obtained from the zebrafish gene collection (ZGC:55844). *cdc14b_tv1* was sub-cloned into the pCS2+ vector with or without sequences encoding a 5′GFP epitope tag.

Quantitative RT-PCR

Primers used for *cdc14b_tv1* and *cdc14b_tv2* transcript variants are listed in Table S1 in the supplementary material. The level of expression was normalized to that of *actin*.

Morpholino and mRNA injections

Three antisense MOs (Gene Tools, Philomath, OR, USA) were designed to target *cdc14b* isoforms: MO1-*cdc14b* (MORPH1734, 5′-CACATGACTGTTGGAAAAGAACAGG-3′), MO2-*cdc14b* (MORPH1736, 5′-CTCGCTTCAACTAAAAACAAAGAGC-3′) and MO3-*cdc14b* (MORPH1735, 5′-TTTGCAGCAGAAGCGGTACAGCATG-3′) (see Fig. S1 in the supplementary material).

For the rescue and protein localization, synthetic mRNAs from *cdc14b_tv1* and *centrin* (gift from Adrian Salic) were made by in vitro transcription using the mMessage mMachine System kit (Ambion, Austin, TX, USA).

Histology

Embryos fixed at 2.5 days post fertilization (dpf) in 4% paraformaldehyde were dehydrated, progressively infiltrated and embedded in JB-4 plastic resin (Polysciences, Warrington, PA, USA). Sections (5 μm) through the kidney were cut using a microtome (Leica RM2265) and stained with 0.5% Toluidine Blue.

Whole-mount in situ hybridization and immunohistochemistry

Embryos and larvae were fixed in 4% paraformaldehyde overnight. Permeabilization was carried out using Proteinase K (10 μg/ml, Roche, Mannheim, Germany). For whole-mount in situ hybridization, embryos and larvae were hybridized overnight at 68°C with the following digoxigenin-labelled probes: *cdc14b_tv1*, *cdc14b_tv2*, *nkx2.5* (Chen and Fishman, 1996), *foxa3* (Odenthal and Nusslein-Volhard, 1998), *southpaw* (Long et al., 2003), *insulin* (Milewski et al., 1998), *no tail* (Schulte-Merker et al., 1994), *myo7a* (Ernest et al., 2000), *erm1* (Munchberg et al., 1999), *pea3* (Munchberg et al., 1999) and *pax2a* (Krauss et al., 1991). Detection and staining were carried out as previously described (Thisse and Thisse, 2008). For immunohistochemistry, embryos were incubated with the following primary antibodies: rabbit anti-GFP (1:500, Torrey Pines Biolabs, East Orange, NJ, USA), mouse anti-acetylated tubulin (1:250, Sigma-Aldrich, St Louis, MO, USA), mouse anti-TAT1 (1:250) (Woods et al., 1989), mouse anti-ZO-1 (1:250, Zymed laboratories, San Francisco, CA, USA) and mouse anti-γ-tubulin (1:500, Sigma-Aldrich, St Louis, MO, USA). Secondary antibodies were goat anti-rabbit or goat anti-mouse (Invitrogen, Carlsbad, CA, USA). F-actin staining was carried out using Alexa-fluor 594 phalloidin (2.5 μM, Invitrogen, Carlsbad, CA, USA) and nuclei were counterstained with TOPRO-3 (Molecular Probes, Eugene, OR, USA).

The ApopTag Peroxidase In Situ Apoptosis Detection Kit (Chemicon, Temecula, CA, USA) was used for the TUNEL assay.

Imaging

Images were acquired using an Imager Z1 compound microscope and AxioVision software (Zeiss, Oberkochen, Germany) (in situ hybridization, sections) or Astro IIDC software (Aupperle Services and Contracting, Calgary, Canada) (movies) and with an LSM510 inverted confocal microscope (Zeiss, Oberkochen, Germany) (immunohistochemistry). Cilia length and pronephric duct diameter were measured following acquisition of *z*-stacks and reconstruction using the LSM Image acquisition software (Version 4.2.0.121, Zeiss, Oberkochen, Germany). Particle path tracking and average intensity per pixel were determined using the Metamorph software (Version 7.1.3.0, Molecular Devices, Silicon Valley, CA, USA).

RESULTS

Cloning and expression pattern of *cdc14* genes

We identified three zebrafish *cdc14* paralogous genes, *cdc14a1* (NM_201149.1, zgc:63654, chromosome 2), *cdc14a2* (NM_001128538, chromosome 22) and *cdc14b* (NM_200179.1, zgc:55844, chromosome 8) (see Figs S1, S2 in the supplementary material), from a BLAST search of the *Ensembl* database using the sequence of *S. pombe* Cdc14 phosphatase, Clp1. Alignment of each zebrafish Cdc14 with CDC14 phosphatases from other organisms showed high sequence identity between the N-terminal catalytic domains and significant divergence among the C termini (see Fig. S3 in the supplementary material). Using RT-PCR from a 24 hpf cDNA library, at least two transcript variants were detected for *cdc14a1*, one for *cdc14a2* and two for *cdc14b* (see Fig. S1 in the supplementary material). Additional transcripts might be expressed. As redundancy is likely to exist between the *cdc14a* genes, we focused our functional studies on *cdc14b*.

Quantitative RT-PCR and in situ hybridization revealed that *cdc14b_tv1* and *cdc14b_tv2* mRNAs were maternally provided and ubiquitously expressed throughout embryonic and early larval development (see Fig. S4 in the supplementary material; data not shown).

Characterization of Cdc14B function

To investigate the function of Cdc14B during embryogenesis, we purchased a mutant line from Znomics (Portland, OR, USA), designated *vu426*, carrying a 7 kb retroviral insertion in the first intron of *cdc14b* sequence (see Fig. S1 in the supplementary material). This insertion was located upstream of both *cdc14b* isoform start codons. Quantitative RT-PCR at 10 hpf revealed that the expression of *cdc14b* was downregulated in the homozygous *cdc14b*$^{vu426/vu426}$ mutants when compared with wild-type embryos (Fig. 1A). *cdc14b_tv1* expression was reduced by ~50%, whereas that of *cdc14b_tv2* was diminished by about 25%. However, this decrease in *cdc14b* expression did not lead to an overt morphological phenotype (Fig. 1B,C).

We therefore employed three MOs to inhibit the function of Cdc14B during embryogenesis (see Fig. S1 in the supplementary material): MO1-*cdc14b* was designed to interfere with splicing of both *cdc14b_tv1* and *cdc14b_tv2* transcripts. MO2-*cdc14b* and MO3-*cdc14b* were designed to prevent translation of *cdc14b_tv1* and *cdc14b_tv2*, respectively. A dose series revealed that, whereas injections of low MO dose at the one-cell stage resulted in no overt morphological defects, injections of 4.5 ng, 3.5 ng and 8.5 ng of MO1-, MO2- and MO3-*cdc14b*, respectively, all produced similar phenotypes, which are described below. These doses were used throughout the experiments unless otherwise specified. The effect of MO1-*cdc14b* on *cdc14b* expression was monitored over time (Fig. 1F): wild-type transcripts were almost completely depleted at 10 hpf, but were detectable again from 1 dpf, indicating that from this stage, loss of Cdc14B function was incomplete. Sequencing of the aberrant transcripts from the embryos injected with MO1-*cdc14b* revealed that the fifth exon, predicted to encode a critical

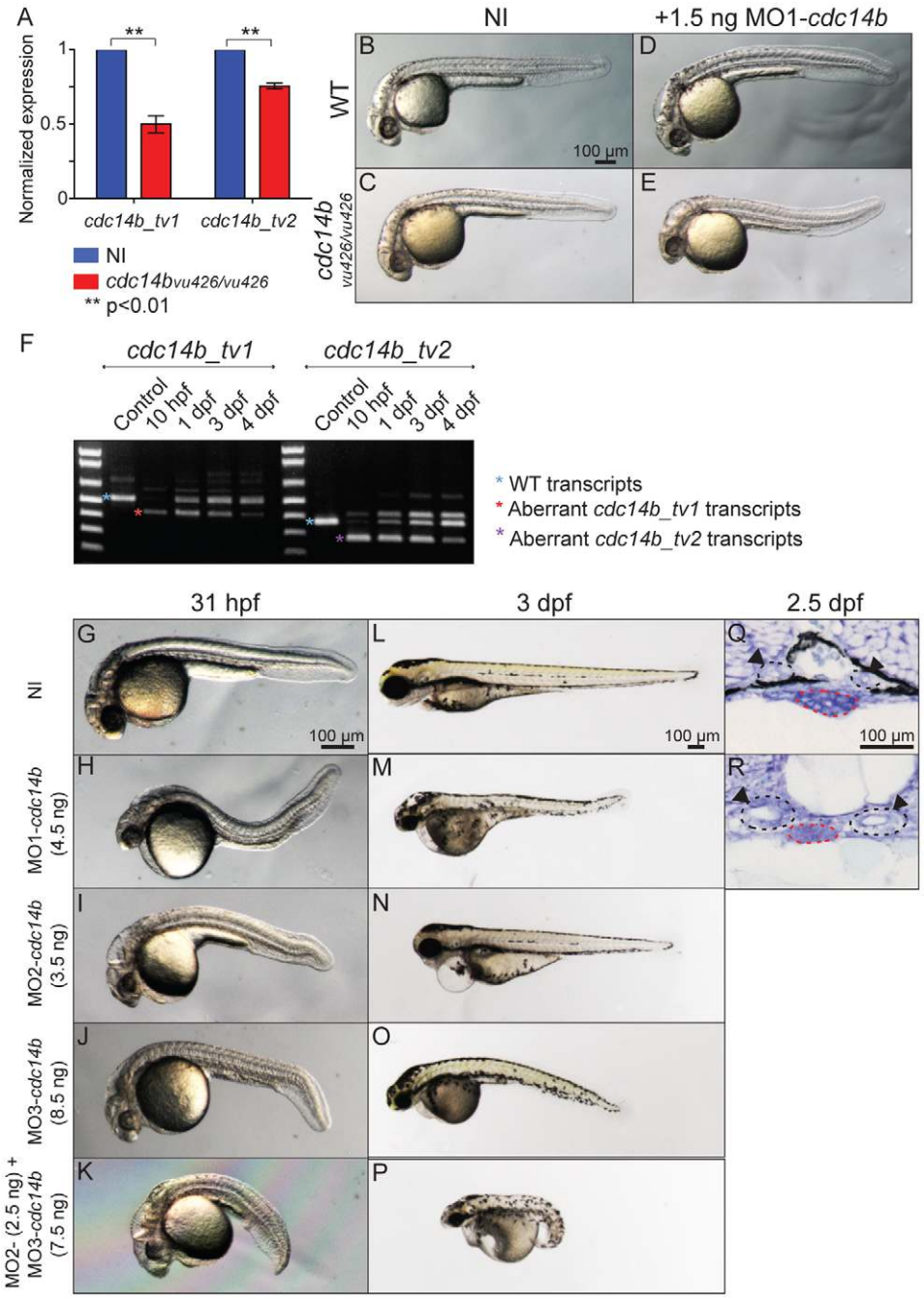

Fig. 1. Morphological phenotype resulting from Cdc14B loss of function. (**A**) Quantitative RT-PCR comparing levels of *cdc14b_tv1* and *cdc14b_tv2* expression in wild-type and *cdc14b*^{vu426} homozygous mutant zebrafish embryos at 10 hpf. Data are mean ± s.e.m. Statistics were carried out using Student's *t*-test. (**B-E**) Wild-type (B,D) and *cdc14b*^{vu426} homozygous mutant (C,E) non-injected (NI) control embryos (B,C) and injected with 1.5 ng of MO1-*cdc14b* (D,E). (**F**) RT-PCR showing the efficiency of 4.5 ng MO1-*cdc14b*. (**G-P**) Non-injected control and *cdc14b* MO-injected embryos/larvae at 31 hpf (G-K) and 3 dpf (L-P). (**Q**,**R**) Sections (5 µm) through the kidney of non-injected control (Q) and MO1-*cdc14b*-injected (R) larvae at 2.5 dpf. The medial tubules (arrowheads) and the gut are outlined in black and red, respectively.

region of the catalytic domain (see Fig. S3 in the supplementary material) (Gray et al., 2003) was spliced out. This suggested that the aberrant transcripts encoded non-functional proteins.

Following injection of each *cdc14b* MO, no obvious morphological phenotype was observed prior to gastrulation, probably due to maternal contribution (see Fig. S4A,B in the supplementary material). By 24 hpf, all *cdc14b*-deficient embryos, referred to as *cdc14b* morphants, presented numerous morphological abnormalities, including hydrocephaly and dorsally or ventrally curved body (Fig. 1G-K). These defects persisted through later stages and from 3 dpf, kidney cysts also became apparent (Fig. 1L-R). Interestingly, the *cdc14b* morphant larvae did not display a strong body axis curvature as seen in zebrafish cilia mutants (Cao et al., 2010; Omori et al., 2008; Sullivan-Brown et al., 2008; Tsujikawa and Malicki, 2004; Zhao and Malicki, 2007). However, this weaker phenotype has previously been observed when MOs against genes encoding cilia proteins were injected (Ferrante et al., 2009; Hurd et al., 2010; Ko et al., 2010; Tsujikawa and Malicki, 2004). This difference in the phenotypes is probably due to the decreased efficiency of the MOs by this time in development. In addition, the size of the body, eyes and ears was reduced. Interestingly, low doses of MO1-*cdc14b*, which did not give rise to morphological defects when injected in wild-type embryos, led to a phenotype resembling that of *cdc14b* morphants when injected in *cdc14b*$^{vu426/vu426}$ embryos (Fig. 1D,E). This is consistent with the notion that the *vu426* allele is hypomorphic and provides further support for the specificity of MO1.

To understand the mechanism underlying the reduced size of the embryos deficient for *cdc14b*, we looked at apoptotic cell death in the tail of *MO1-cdc14b* morphants at 27 hpf. TUNEL analysis revealed increased apoptosis in the morphants in comparison to non-injected control siblings (see Fig. S5A in the supplementary material). To assess whether cell death, due to either MO toxicity or Cdc14B loss of function, contributed to the morphological defects observed in *cdc14b* morphants, we used *p53* zebrafish mutants, in which apoptosis is significantly suppressed (Berghmans et al., 2005). When each *cdc14b* MO was injected into embryos produced by $tp53^{zdf1/zdf1}$ parents, *cdc14b* morphants still displayed hydrocephaly, curved bodies, smaller eyes and ears and, although less pronounced, a shorter body (see Fig. S5B-K in the supplementary material). Therefore, excessive apoptotic cell death was unlikely to explain the morphological defects in *cdc14b*-deficient embryos, although it was in part responsible for the reduced morphant body size. We next analyzed the number of mitotic figures in the tail of *MO1-cdc14b* morphants at 27 hpf. Cell proliferation was diminished in *cdc14b* morphant embryos when compared to non-injected control siblings (see Fig. S5L in the supplementary material), and thus could also contribute to the reduced size of *cdc14b*-deficient embryos.

Cdc14B acts to establish left-right (LR) asymmetry

Hydrocephaly, curved body and kidney cysts are often associated with ciliogenesis defects in zebrafish (Wessely and Obara, 2008). Zebrafish cilia mutants also exhibit improper specification of LR asymmetry. Thus, we examined *cdc14b* morphants for defects in

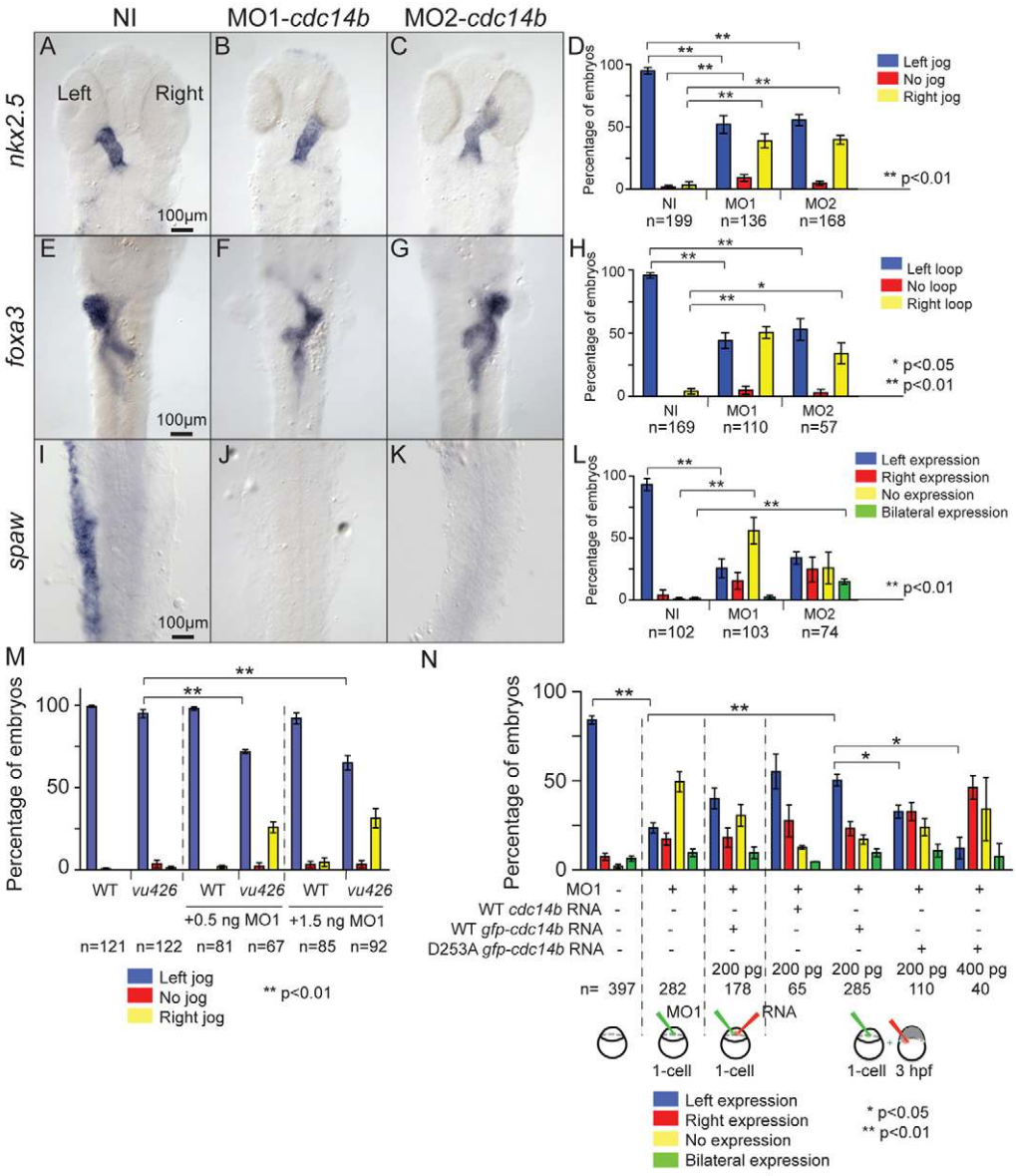

Fig. 2. Effect of inhibition of Cdc14B function on LR asymmetry. (**A-L**) In situ hybridization and expression pattern quantification in non-injected and *cdc14b* MO-injected zebrafish embryos of *nkx2.5* (A-D), *foxa3* (E-H) and *spaw* (I-L) at 31 hpf, 50 hpf and 19 hpf, respectively. (**M**) Quantification of LR asymmetry defects in non-injected and 0.5 ng or 1.5 ng MO1-*cdc14b*-injected wild-type and $cdc14b^{vu426}$ homozygous mutant embryos at 31 hpf using *cmlc2:GFP* transgene. (**N**) Rescue of the LR asymmetry phenotype in MO1-*cdc14b*-injected embryos. LR asymmetry defects were quantified using *spaw* expression pattern at 18 hpf. Numbers of embryos analyzed are indicated (*n*). Data are mean ± s.e.m. Statistics were carried out using Student's *t*-test (D,H,L,M) and paired Student's *t*-test (N), and are only presented for the left-sided heart class in M and the *spaw* left expression class in N.

LR asymmetry using markers for asymmetrically positioned organs. Expression of heart markers *nkx2.5* and *cmlc2* (Chen and Fishman, 1996; Yelon et al., 1999) at 31 hpf showed that, as expected, the heart tube shifted to the left in most uninjected control embryos, whereas in the *cdc14b* morphants the shifting direction was random (Fig. 2A-D; see Fig. S6A-D in the supplementary material). Expression patterns of *foxa3* and *insulin*, markers of the visceral organs (Milewski et al., 1998; Odenthal and Nusslein-Volhard, 1998), at 49 hpf, indicated that gut looping and localization of the liver and pancreas were also randomized in *cdc14b* morphants (Fig. 2E-H; see Fig. S6E-H in the supplementary material). We analyzed the expression of the earliest known marker asymmetrically expressed, *southpaw* (*spaw*), encoding a Nodal-related ligand (Long et al., 2003), at 18 hpf. Whereas *spaw* was expressed in the left lateral plate mesoderm (LPM) in the uninjected control embryos, in the *cdc14b* morphants its expression was seen either in the left LPM, the right LPM, both sides of the LPM or was absent (Fig. 2I-L). Injection of synthetic *cdc14b* RNA (up to 0.4 ng) did not alter expression of *spaw* (see Fig. S6I in the supplementary material).

As injection of low doses of MO1-*cdc14b* in *cdc14b*$^{vu426/vu426}$ mutant embryos could phenocopy the morphological defects manifested by *cdc14b*-depleted embryos, we wanted to know whether LR asymmetry defects could also be seen in the injected mutants. Analyzing heart location, the non-injected *cdc14b*$^{vu426/vu426}$ mutants did not display LR asymmetry defects. However, injection of low doses of MO1-*cdc14b* induced this defective phenotype in mutant, but not in wild-type embryos (Fig. 2M).

To verify the specificity of the LR asymmetry phenotype in the *cdc14b* morphants, we performed rescue experiments using synthetic *cdc14b_tv1* mRNAs and *spaw* expression at 18 hpf as a read-out. MO1-*cdc14b* was injected at the one-cell stage alone or co-injected with the *cdc14b_tv1* mRNAs. The expression of *spaw* exclusively in the left LPM was restored in a significant fraction of co-injected embryos in comparison with the embryos injected with MO1-*cdc14b* only (Fig. 2N).

Mechanisms leading to LR asymmetry have been characterized in many species (Basu and Brueckner, 2008). In zebrafish, the ciliated KV is the organ that establishes LR asymmetry (Essner et al., 2005). Within the KV, beating cilia generate a directional fluid flow that results in asymmetric gene expression. To determine whether Cdc14B was required for LR asymmetry in the KV, we performed a different type of rescue experiment. MO1-*cdc14b* was first injected at the one-cell stage. While some embryos were kept as controls, the rest were injected into the yolk with *cdc14b_tv1* or *cdc14b_tv1-gfp* (which encodes a Cdc14B C-terminal GFP fusion) mRNAs at 3 hpf, after the yolk syncytial layer became separated from the embryo proper (Kimmel and Law, 1985). By injecting into the yolk syncytium at 3 hpf, we aimed to target the mRNAs specifically to the dorsal forerunner cells (DFCs) that give rise to the KV (Cooper and D'Amico, 1996; Melby et al., 1996). Indeed, between 3 and 4 hpf, only the DFCs share cytoplasmic bridges with the yolk cell where the mRNAs are injected. Aberrant *spaw* expression in the *cdc14b* morphants was partially suppressed after *cdc14b_tv1* or *cdc14b_tv1-gfp* mRNAs were injected at 3 hpf (Fig. 2N). The rescue experiments, in addition to similar LR asymmetry defects produced by injection of three different MOs and by injection of low doses of MO1-*cdc14b* in *cdc14b*$^{vu426/vu426}$ mutant embryos, led us to conclude that the LR asymmetry phenotype in *cdc14b* morphants is specifically due to a loss of Cdc14B function rather than non-specific activity of the MOs.

As Cdc14 function in cell cycle control relies on its phosphatase activity (Trinkle-Mulcahy and Lamond, 2006), we investigated whether this activity was necessary for the role of Cdc14B in establishing LR asymmetry. We injected MO1-*cdc14b* at the one-

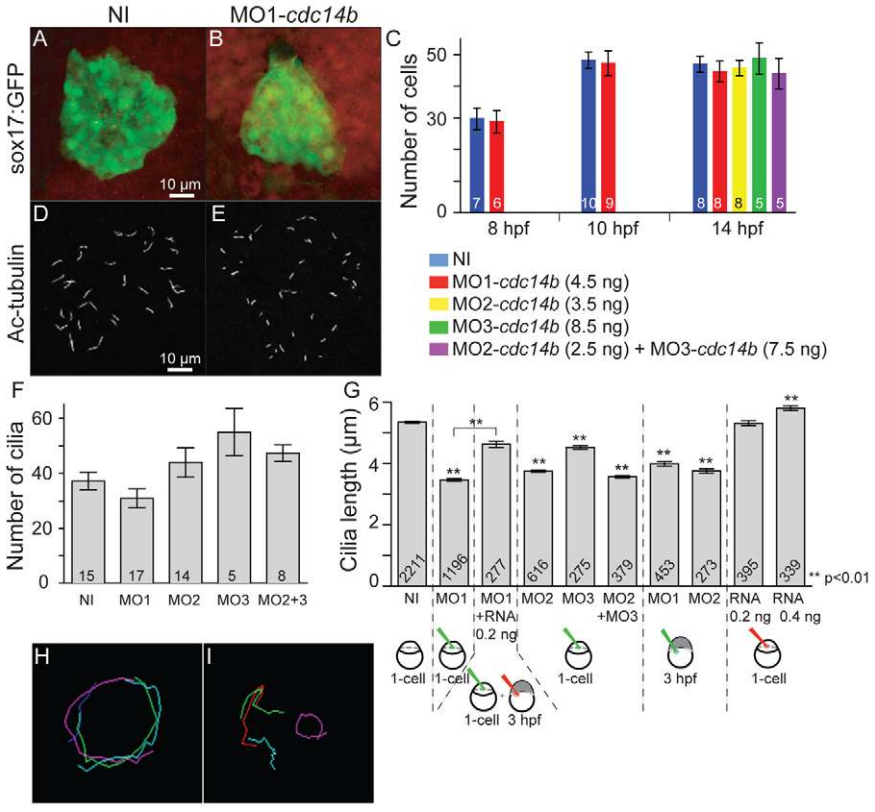

Fig. 3. Cdc14B loss- and gain-of-function effect on the KV. (**A**,**B**) KV at 10 hpf visualized using Sox17-GFP. (**C**) The number of cells in the KV was determined in non-injected and *cdc14b* MO-injected zebrafish embryos at the indicated times. (**D**,**E**) Cilia in the KV at 14 hpf visualized with an anti-acetylated-tubulin (Ac-tubulin) antibody. (**F**,**G**) Cilia numbers (F) and cilia length (G) were determined at 14 hpf. The numbers of embryos (C,F) and cilia (G) analyzed are indicated. Data are mean ± s.e.m. Statistics were carried out using Student's *t*-test. Unless otherwise shown, statistics were calculated against the NI sample. (**H**,**I**) Particle paths in the KV of a single non-injected (H) or MO1-*cdc14b*-injected (I) embryo at 14 hpf. Three embryos were analyzed per condition.

cell stage and then, at 3 hpf, synthetic *cdc14b_tv1* mRNA carrying a mutation in the catalytic domain such that it encoded a phosphatase dead protein (D253A) (Wolfe et al., 2006). Injection of the mutated mRNAs in the morphant embryos did not rescue the LR asymmetry defect (Fig. 2N), indicating that the phosphatase activity of Cdc14B was required for its role in establishing LR asymmetry. Injection of the mutated mRNA alone (up to 0.4 ng) did not affect LR asymmetry establishment (see Fig. S6I in the supplementary material), suggesting that at this level of expression the phosphatase-dead protein did not exert a dominant-negative activity.

Cellular mechanism of Cdc14B action in LR asymmetry

To identify the cellular basis of the LR asymmetry defect in the *cdc14b* morphants, we first examined the integrity of the midline as disruption of this structure can lead to LR asymmetry defects via mis-localization of the cues defining the left and right sides (Bisgrove et al., 2000; Danos and Yost, 1996). Similar expression of *no tail* (Schulte-Merker et al., 1994) in the notochord of uninjected control siblings and *cdc14b*-deficient embryos at 8 hpf and 10 hpf (see Fig. S7A-D in the supplementary material) suggested that the midline was not affected.

We then examined KV morphogenesis. The KV had normal size and shape, and was properly inflated at 14 hpf (Fig. 3A,B; see Fig. S7E,F in the supplementary material) (Oteiza et al., 2008). Furthermore, *sox17*, a marker of the DFCs that give rise to the KV, as well as *no tail* (Melby et al., 1996; Schulte-Merker et al., 1994) were correctly expressed in the KV at 10 hpf and 8.5 hpf, respectively (Fig. 3A,B; see Fig. S7A,B in the supplementary material).

As Cdc14B is implicated in cell cycle control, we next investigated whether the number of cells that make up the KV was reduced in the *Tg[sox17:GFP]* embryos injected with *cdc14b* MOs at three developmental time points: (1) at 8 hpf, when the KV is not formed yet and the DFCs are about to divide, (2) at 10 hpf, when the KV is forming and cell division has occurred and (3) at 14 hpf, when the KV is fully formed and functional, as described by previous studies (Amack et al., 2007; Cooper and D'Amico, 1996). No significant differences were observed in the number of KV cells between uninjected control embryos and *cdc14b* morphants at any of these stages (Fig. 3C).

Finally, we examined cilia of the fully formed KV in the *cdc14b* morphants at 14 hpf. The correct number of KV cilia were present (Fig. 3D-F) and they could beat in the morphants, suggesting that their structure was not significantly affected (see Movies 1 and 2 in the supplementary material). However, our morphometric analyses indicated that the length of KV cilia was significantly reduced in the *cdc14b* morphants compared with that observed in uninjected control embryos (Fig. 3D,E,G; see Fig. S7G-J in the supplementary material). To show that the *cdc14b* MOs had a specific effect on KV ciliated cells, we injected MO1-*cdc14b* and MO2-*cdc14b* at 3 hpf to target the DFCs that will form the KV. We found that in these *cdc14b*-depleted embryos, the length of the KV cilia was also diminished (Fig. 3G). Moreover, using the same principle of rescue with sequential injection of MO1-*cdc14b* at the one-cell stage and *cdc14b_tv1-gfp* RNA at 3 hpf, we showed that the decrease in length of the KV cilia was specifically due to Cdc14B loss of function. Interestingly, in gain-of-function experiments, whereas 0.2 ng of *cdc14b_tv1-gfp* mRNAs did not produce a difference in the length of the KV cilia (Fig. 3G; see Fig. S7K in the supplementary material), 0.4 ng was sufficient to cause a significant increase in cilia length (Fig. 3G; see Fig. S7L in the supplementary material). However, this increase in cilia length was not associated with a LR asymmetry phenotype (see Fig. S6I in the supplementary material).

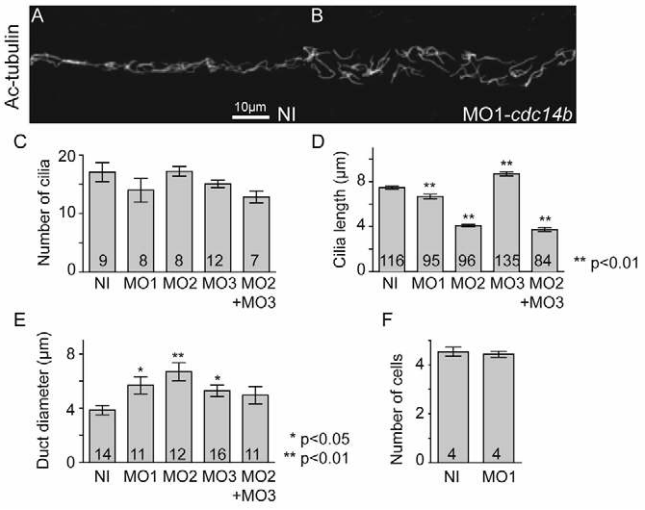

Fig. 4. Cdc14B loss-of-function effect on kidney cilia. (**A**,**B**) Cilia in the kidney duct at 27 hpf visualized with an anti-Ac-tubulin antibody. (**C**,**D**) Cilia numbers (C) and length (D) were determined at 27 hpf. (**E**) Kidney duct diameter was measured at 27 hpf. (**F**) Number of cells in sections of the kidney tubules at 2.5 dpf. The numbers of embryos (C,E,F) and cilia (D) analyzed are indicated in each column. Data are mean ± s.e.m. Statistics were carried out using Student's *t*-test.

Recent studies indicate that cilia length is important for normal fluid flow in the KV (Neugebauer et al., 2009). Tracking of particle paths within the KV confirmed that fluid flow was disrupted in the KV of *cdc14b*-deficient embryos (Fig. 3H,I), presumably owing to their shorter length. Altogether, these results suggest that Cdc14B is involved in LR asymmetry establishment via a role in ciliogenesis.

Cdc14B loss of function affects several types of cilia

The ubiquitous expression of *cdc14b* and the morphological phenotype of the *cdc14b* morphants suggested that other types of cilia could also be affected. Thus, we examined a structurally different type of motile cilia in the posterior kidney duct of uninjected control and MO1-*cdc14b*-injected embryos at 27 hpf. As in the KV, these cilia were present in the correct number (Fig. 4A-C). This observation also implied a correct number of ciliated cells, as cells are monociliated in the posterior kidney duct (Liu et al., 2007b). We confirmed that the number of cells was unaffected in the kidney duct of the *cdc14b* morphants at 2.5 dpf (Fig. 4F) (Sullivan-Brown et al., 2008). However, the kidney cilia were significantly shorter (Fig. 4D). Defects in cilia can result in fluid flow disruption causing enlargement of the duct (Kramer-Zucker et al., 2005; Sun et al., 2004). Indeed, the duct diameter was significantly enlarged in the *cdc14b*-deficient embryos compared with that of uninjected control siblings (Fig. 4A,B,E).

Next, we investigated primary cilia in the five sensory patches of the inner ear (anterior, lateral and posterior cristae, utricular and saccular maculae) (Whitfield et al., 2002) of 4 dpf larvae injected with MO1-*cdc14b*. Again, we found a significant decrease in the length of the kinocilia in the saccular macula and in the other

sensory patches but also a decrease in their number (Fig. 5A-D; see Fig. S8A-C in the supplementary material). To clarify if the decrease in kinocilia number was due to a decrease in the number of hair cells from which kinocilia emanate, we analyzed the size of the sensory patches using *myo7a*, a marker of the hair cell terminal differentiation (Ernest et al., 2000). We observed a slight decrease in the size of the five sensory patches in the *cdc14b* morphants (Fig. 5E,F) and a diminution in the number of cells counted in the saccular macula (Fig. 5G). All five sensory patches consist of a double-layered epithelium that results from the asymmetric division of precursor cells into supporting cells and hair cells (Haddon et al., 1998). When we analyzed the structure of the maculae, we found that the *cdc14b*-deficient larvae displayed a double-layered epithelium similar to that of non-injected control siblings (Fig. 5H,I), and also that the ratio of the hair cell to supporting cell numbers was comparable in *cdc14b* morphant and control larvae (Fig. 5J). This indicated that a cell proliferation defect occurred prior to formation of the double-layered epithelium leading to a reduced number of precursor cells and thereby a diminished number of hair cells. Confirming this, we found that, as previously described (Platt, 1993; Sobkowicz et al., 1995), each kinocilium in the *cdc14b* morphant larvae was always associated with an actin-rich structure called stereocilia at the surface of the hair cells (Fig. 5K). Altogether, these results suggest that Cdc14B can affect ciliogenesis independently of its impact on cell proliferation.

Cdc14B is unlikely to regulate centriole migration to the membrane

To further examine the role of Cdc14B during ciliogenesis, we analyzed its subcellular localization. Owing to the lack of specific antibody, we injected in the one-cell stage embryos *cdc14b_tv1-gfp* mRNAs, as previously used for the rescue experiments, and monitored the dynamic localization of the protein in embryos at 8 hpf. Cdc14B was restricted to the nucleolus during interphase and was released in the cytoplasm during mitosis (Fig. 6A), consistent with the localization of Cdc14B from other vertebrate organisms (Berdougo et al., 2008; Cho et al., 2005; Kaiser et al., 2002; Mailand et al., 2002; Schindler and Schultz, 2009a; Wu et al., 2008). Also consistent with previous studies (Berdougo et al., 2008; Buffone et al., 2009; Schindler and Schultz, 2009a), we observed Cdc14B at the chromosomes and the mitotic spindle. However, we did not detect Cdc14B at centrosomes (Buffone et al., 2009; Cho et al., 2005; Wu et al., 2008) or at basal bodies, suggesting that Cdc14B affected ciliogenesis from another location.

In order to define the step of ciliogenesis regulated by Cdc14B, we first analyzed centriole migration to the membrane in the epithelial cells of the posterior kidney duct at 27 hpf. Although MO1-*cdc14b* morpholinos were not 100% efficient at 27 hpf, we reasoned that if cilia were shorter in the kidney, the reduction in *cdc14b* expression must be sufficient to disrupt ciliogenesis and therefore to impair migration of the centriole at the apical membrane if this process was regulated by Cdc14B. The centrioles

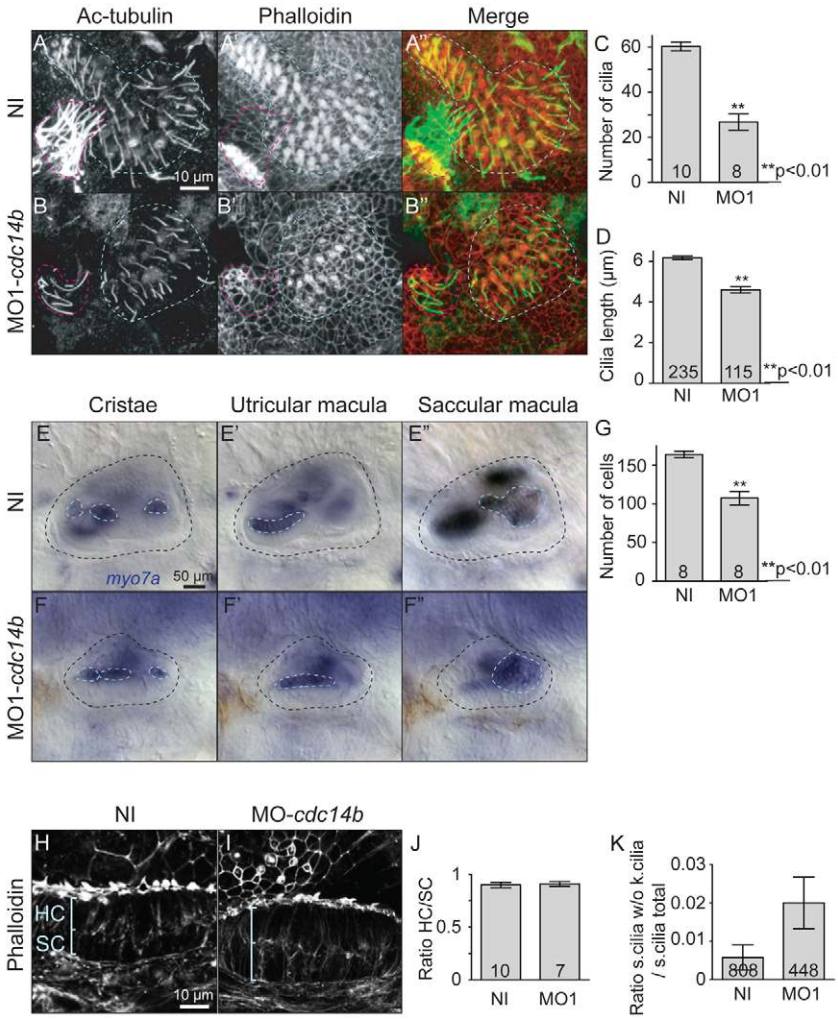

Fig. 5. Cdc14B loss-of-function effect on inner ear kinocilia. (**A-B″**) Saccular macula at 4 dpf visualized with phalloidin and an anti-Ac-tubulin antibody. The latter structure is outlined in blue; the lateral crista is outlined in red. (**C**,**D**) Cilia numbers (C) and length (D) were determined at 4 dpf. (**E-F″**) *myo7a* in situ hybridization in the inner ear at 4 dpf. (**G**) The number of cells in the saccular macula was determined in non-injected and MO1-*cdc14b*-injected larvae at 4 dpf. (**H**,**I**) Structure of the utricular macula in non-injected (H) and MO1-*cdc14b*-injected (I) larvae at 4 dpf visualized by phalloidin. (**J**) Ratio between the numbers of hair cells (HC) and supporting cells (SC) at 4 dpf. (**K**) Ratio between the numbers of stereocilia (s.cilia) not associated to kinocilia (k.cilia) and the total number of stereocilia. The numbers of larvae (C,G,J), cilia (D) and hair cells (K) analyzed are indicated. Data are mean ± s.e.m. Statistics were carried out using Student's *t*-test.

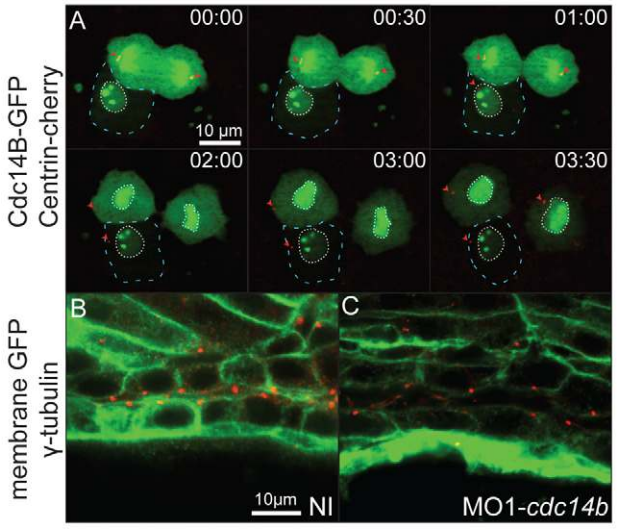

Fig. 6. Analysis of Cdc14B function during ciliogenesis.
(**A**) Dynamic distribution of Cdc14B during cell division at 8 hpf. The embryo was injected with synthetic *cdc14b_tv1-GFP* (green) and *centrin-cherry* (red) RNAs. Dashed lines outline a cell in interphase. (Top cell) A dividing cell proceeding through anaphase (00:00-00:30), telophase (1:00-2:00) and interphase (3:00-3:30). Arrowheads indicate the centrioles. Dotted lines outline the nuclear envelope. (**B**,**C**) Positioning of the centrioles in the posterior kidney duct at 27 hpf in non-injected (B) and MO1-*cdc14b*-injected (C) embryos visualized with an anti-γ-tubulin antibody (red) and phalloidin (green).

appeared normally positioned at the apical side of the epithelial cells in distended kidney duct of both non-injected and MO1-*cdc14b* injected embryos (Fig. 6B,C). In addition, kinocilia emanated from the membrane rather than from the cytoplasm when viewed in cross-section of the sensory patches (data not shown) in morphant larvae. Altogether, we interpret these results to mean that Cdc14B is unlikely to regulate the first steps of ciliogenesis involving movement of the centrioles/basal bodies to the membrane.

Role of Cdc14B in regulation of cilia length

The correct number of cilia in the KV as well as the posterior kidney duct suggested that nucleation of the cilia occurred properly in *cdc14b*-depleted embryos. Therefore, we reasoned that Cdc14B might influence cilia length control. The FGF pathway modulates cilia length via maintenance of a transcriptional network leading to the expression of intraflagellar transport (IFT) proteins required for cilia growth (Neugebauer et al., 2009). Therefore, we tested whether Cdc14B acted in the same or parallel pathway to FGF to regulate cilia length. Our analysis of *cdc14b* morphants revealed that two FGF target genes, *erm1* and *pea3* (Raible and Brand, 2001; Roehl and Nusslein-Volhard, 2001), were correctly expressed in the DFCs at 8.5 hpf (Fig. 7A-D) and that *pax2a*, another FGF target gene (Hans et al., 2004; Phillips et al., 2001; Reifers et al., 1998), was also normally expressed in the eyes, the midbrain-hindbrain boundary, the otic placode and the developing pronephros at 17.5 hpf (Fig. 7E,F; data not shown).

Next, we analyzed the effect of both Cdc14B and FGF8 loss of function on cilia length. To this end, we used a null allele of *fgf8*, *x15* (Kwon and Riley, 2009), and we injected a low-dose of MO1-*cdc14b* in *fgf8/acerebellar*$^{x15/x15}$ (*fgf8/ace*$^{x15/x15}$) homozygous

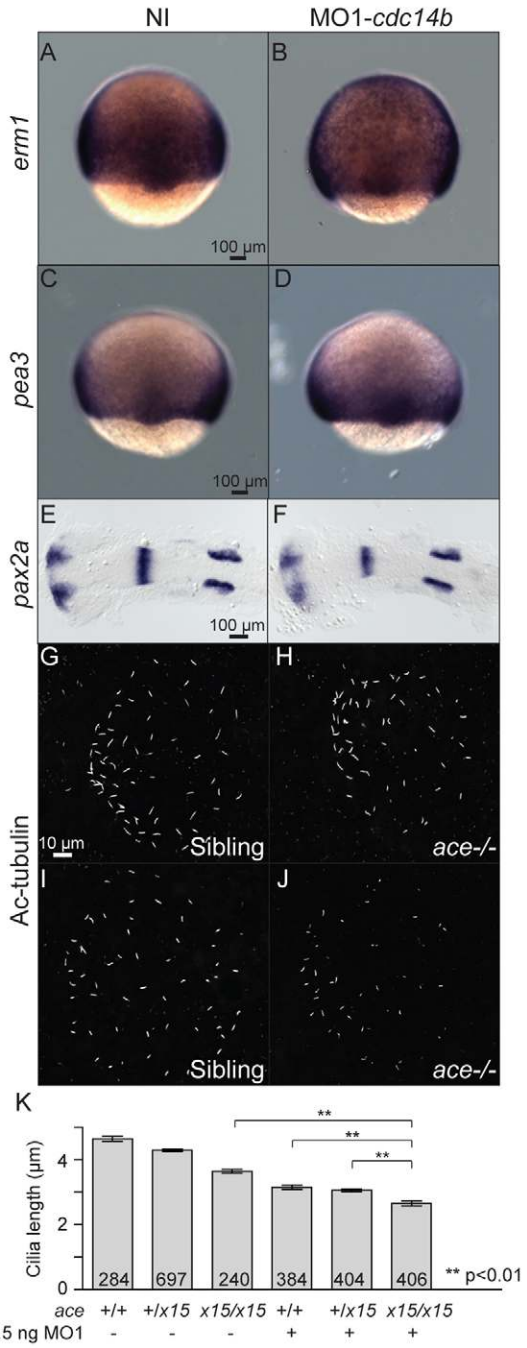

Fig. 7. Interaction between the FGF pathway and Cdc14B.
Expression pattern of *erm1* (**A**,**B**) and *pea3* (**C**,**D**) at 8 hpf, and *pax2a* (**E**,**F**) at 17 hpf. (**G-J**) KV cilia in siblings and *fgf8/ace*^{x15} homozygous mutant embryos, non-injected (G,H) or injected with MO1-*cdc14b* (I,J) at 14 hpf visualized with an anti-Ac-tubulin antibody. (**K**) Cilia length was determined at 14 hpf. The numbers of cilia analyzed are indicated. Data are mean ± s.e.m. Statistics were carried out using Student's *t*-test.

mutants and siblings. In contrast to what was previously described (Neugebauer et al., 2009), at 14 hpf, KV cilia were shorter in non-injected *fgf8/ace*$^{x15/x15}$ mutants in comparison with their siblings (Fig. 7G,H,K). This could be explained by the fact that we used a different *fgf8/ace* mutant allele. In embryos injected with low doses of MO1-*cdc14b*, the length of KV cilia was diminished in siblings

and even further reduced in the *fgf8/ace*$^{x15/x15}$ homozygous mutant embryos (Fig. 7I-K). The fact that loss of Cdc14B function enhanced the effect of the loss of FGF signaling on KV cilia length, in addition to the normal expression of FGF targets in *cdc14b*-deficient embryos, suggested that Cdc14B and the FGF pathway act in parallel to regulate cilia length.

Microtubule acetylation is required to maintain cilia. Using similar conditions to acquire images of KV cilia stained with an anti-acetylated-tubulin antibody in morphant and non-injected control embryos at 14 hpf, we observed that the average intensity of microtubule acetylation was reduced in the morphants (Fig. 8A-C). These results provide a plausible mechanism whereby Cdc14B could regulate cilia microtubule stability. However, although statistically significant, the observed decrease in the acetylation level of the cilia microtubules was small and might be insufficient on its own to account for the shorter cilia in *cdc14b* morphant embryos.

DISCUSSION

Here, we examined the role of Cdc14B, one of two Cdc14 family members in vertebrates, during zebrafish embryonic development. Using an insertional mutant and three different antisense MOs to impair Cdc14B function, we found and confirmed by rescue and gain-of-function experiments, that Cdc14B plays an important role in ciliogenesis, and consequently in a number of developmental processes, including LR asymmetry establishment, and kidney and ear development.

Independent functions of Cdc14B in cell division control and ciliogenesis

The Cdc14 phosphatase family is best known for its roles in cell cycle control, especially in mitotic exit (Stegmeier and Amon, 2004). By analyzing concomitantly cilia length and cell number in the KV, in the kidney duct and in the inner ear sensory patches, we were able to show that, in these cases, the function of Cdc14B in ciliogenesis could be dissociated from any potential role in cell division. Thus, Cdc14B appears to be functioning in a new biological process in zebrafish when compared with its established functions in yeasts.

Several explanations can account for the absence of cell cycle defects, despite a significant ciliogenesis defect in some of the tissues we studied in *cdc14b*-deficient embryos: (1) sufficient Cdc14B activity could remain after MO injections for cell division to occur; (2) unknown and non-targeted isoforms of Cdc14B and/or Cdc14A enzymes could compensate for Cdc14B loss of function in mitosis; and/or (3) other phosphatases are responsible for dephosphorylating mitotic proteins and allowing the cell to proceed through M-phase. It is also possible that Cdc14B is required for cell division in a subset of cells but dispensable for a majority of cell divisions in zebrafish.

In the tail as well as in the population of hair cell precursors, we observed a decrease in the number of mitotic figures in *cdc14b*-depleted embryos. This could be due to less proliferation, as discussed above, or delayed cell cycle progression and development. It should also be noted that in *S. pombe*, cells lacking the Cdc14 ortholog Clp1/Flp1 display a reduced length owing to premature entry into mitosis (Cueille et al., 2001; Trautmann et al., 2001). Thus, the diminished size of *cdc14b*-deficient embryos might result from smaller cells. Further study will be required to distinguish between these possibilities and discover whether the role of Cdc14 phosphatases in yeast cell cycle control can be extended to vertebrates.

Function of Cdc14B in ciliogenesis

In yeast, Cdc14 phosphatases are controlled by their subcellular localization and the same is thought to be true of their vertebrate counterparts. During interphase, Cdc14 is sequestered and kept inactive in the nucleolus, whereas it is released and fully active during late stages of mitosis (Trinkle-Mulcahy and Lamond, 2006). Ciliogenesis is a cell cycle-dependent process. During G1, the centriole migrates from the cytoplasm to the apical surface of the cell where it docks to the membrane (Dawe et al., 2007). Elongation of the cilium then occurs. During G2, the cilium retracts and it is absent during the following M-phase. If zebrafish Cdc14B is active only in anaphase, it would probably influence the dynamics of ciliogenesis early in the process. Our analysis of the first steps of ciliogenesis indicates that Cdc14B probably does not influence centriole migration and docking at the membrane (Fig. 6B,C) nor is it required in cilia nucleation. Furthermore, cilia beat in embryos depleted of Cdc14B, suggesting that their structure is relatively intact (see Movies 1 and 2 in the supplementary material). Based on these observations, we propose that Cdc14B regulates cilia elongation and/or maintenance.

Cdc14 proteins function in cell division control via their phosphatase activity. Because overexpression of the wild-type but not phosphatase-dead Cdc14B protein suppressed LR asymmetry defects of the *cdc14b* morphants (Fig. 2N), we conclude that Cdc14B requires its phosphatase activity to establish LR asymmetry. Knowing that the LR asymmetry defect in *cdc14b*-deficient embryos is likely due to the reduced length of the KV cilia, it is expected that Cdc14B affects ciliogenesis via dephosphorylation of substrates yet to be identified. As phosphoregulation is already known to be a key mechanism regulating ciliogenesis (Gerdes et al., 2009), it is reasonable to think that Cdc14 phosphatases evolved to participate in this process.

Proteomic analyses of cilia and flagella in different organisms have revealed the presence of many kinases and phosphatases in these structures (Boesger et al., 2009; Liu et al., 2007a; Ostrowski et al., 2002; Pazour et al., 2005). Notably, phosphatase inhibitor 2

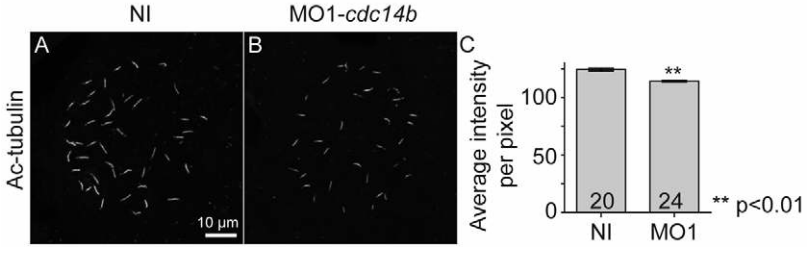

Fig. 8. Cdc14B function in cilia length regulation. (**A**,**B**) KV cilia at 14 hpf visualized with an anti-Ac-tubulin antibody. (**C**) Quantification of the acetylation level in the microtubules of KV cilia in non-injected and MO1-*cdc14b*-injected embryos at 14 hpf. Data are mean ± s.e.m. Statistics were carried out using Student's *t*-test.

has been proposed to promote stability of the cilia via tubulin acetylation of the cilia axoneme due to indirect inhibition of histone/tubulin deacetylases such as HDAC-6 (Wang and Brautigan, 2008). On the contrary, the Aurora A kinase is involved in cilia disassembly via phosphorylation and activation of HDAC-6 (Pugacheva et al., 2007). Interestingly, mammalian CDC14B as well as *S. cerevisiae* Cdc14 have been previously shown to have a role in microtubule stabilization (Cho et al., 2005; Higuchi and Uhlmann, 2005). Although *cdc14b* morphant embryos display a decrease of the acetylation level of cilia microtubules (Fig. 8A-C), we cannot at this point conclude whether the role of Cdc14B in ciliogenesis is limited to this effect.

Several models have been proposed to explain cilia length regulation. One relies on a balance between assembly and disassembly rates of the cilia microtubules (Marshall and Rosenbaum, 2001). Numerous kinases have previously been involved in regulation of cilia/flagella length. In *Chlamydomonas reinhardtii*, *Long Flagella 2* (*LF2*) and *LF4* encode a CDK-related kinase and a MAP kinase, respectively, that are implicated in flagellar length control (Berman et al., 2003; Tam et al., 2007). In zebrafish, a homolog of LF2p, cell cycle-related kinase, was recently implicated in cilia assembly (Ko et al., 2010). Given the affiliation between Cdc14 phosphatases and CDKs, and the fact that LF2p and its homolog localize to the cytoplasm rather than to the cilia/flagella, it will be interesting to test genetic and molecular interactions between these components.

Conservation of Cdc14 phosphatase function

Cilia defects have not been described in *C. elegans* lacking Cdc14, possibly because the role of Cdc14 in ciliogenesis is redundant with other phosphatases in this organism. However, the role of Cdc14B in ciliogenesis might be conserved in other invertebrates or vertebrates. Certainly, the characterization of *cdc14* mutants in *Chlamydomonas reinhardtii* would shed light on the conservation of this function in invertebrates.

We identified three zebrafish *cdc14* genes, two homologs of *cdc14a* and a single *cdc14b* gene, with numerous splice variants. The diversity of *cdc14* transcripts will probably be a complicating factor in the functional analysis of Cdc14 proteins in vertebrate species. Their variable domains might allow specific subcellular localization, substrate interaction or regulation, and, in turn, the evolution of specific functions. In our studies, we simultaneously targeted two major transcripts of *cdc14b* and future studies will be necessary to determine whether they contribute equally to ciliogenesis.

In human cells, Cdc14A localizes to centrosomes (Kaiser et al., 2002; Mailand et al., 2002). It will therefore be interesting to determine whether Cdc14A also participates in ciliogenesis and if its function is redundant with Cdc14B or is independent of Cdc14B. In addition, it will be important to determine whether an imbalance of Cdc14 phosphatase activity underlies or impacts human ciliopathies.

Acknowledgements

The authors thank members of the Gould and Solnica-Krezel labs for many valuable discussions and comments on the manuscript, Dr B. Blanco-Sanchez and Dr T. Whitfield for their advice on the sensory patches study, and the Westerfield lab for reagents. This work was supported by a Martha Rivers Ingram endowment to L.S.K. and the HHMI, of which K.L.G. is an investigator. Deposited in PMC for release after 6 months.

Competing interests statement

The authors declare no competing financial interests.

Supplementary material

Supplementary material for this article is available at
http://dev.biologists.org/lookup/suppl/doi:10.1242/dev.055038/-/DC1

References

Amack, J. D., Wang, X. and Yost, H. J. (2007). Two T-box genes play independent and cooperative roles to regulate morphogenesis of ciliated Kupffer's vesicle in zebrafish. *Dev. Biol.* **310**, 196-210.

Bassermann, F., Frescas, D., Guardavaccaro, D., Busino, L., Peschiaroli, A. and Pagano, M. (2008). The Cdc14B-Cdh1-Plk1 axis controls the G2 DNA-damage-response checkpoint. *Cell* **134**, 256-267.

Basu, B. and Brueckner, M. (2008). Cilia multifunctional organelles at the center of vertebrate left-right asymmetry. *Curr. Top. Dev. Biol.* **85**, 151-174.

Bembenek, J. and Yu, H. (2001). Regulation of the anaphase-promoting complex by the dual specificity phosphatase human Cdc14a. *J. Biol. Chem.* **276**, 48237-48242.

Berdougo, E., Nachury, M. V., Jackson, P. K. and Jallepalli, P. V. (2008). The nucleolar phosphatase Cdc14B is dispensable for chromosome segregation and mitotic exit in human cells. *Cell Cycle* **7**, 1184-1190.

Berghmans, S., Murphey, R. D., Wienholds, E., Neuberg, D., Kutok, J. L., Fletcher, C. D., Morris, J. P., Liu, T. X., Schulte-Merker, S., Kanki, J. P. et al. (2005). tp53 mutant zebrafish develop malignant peripheral nerve sheath tumors. *Proc. Natl. Acad. Sci. USA* **102**, 407-412.

Berman, S. A., Wilson, N. F., Haas, N. A. and Lefebvre, P. A. (2003). A novel MAP kinase regulates flagellar length in Chlamydomonas. *Curr. Biol.* **13**, 1145-1149.

Bisgrove, B. W. and Yost, H. J. (2006). The roles of cilia in developmental disorders and disease. *Development* **133**, 4131-4143.

Bisgrove, B. W., Essner, J. J. and Yost, H. J. (2000). Multiple pathways in the midline regulate concordant brain, heart and gut left-right asymmetry. *Development* **127**, 3567-3579.

Boesger, J., Wagner, V., Weisheit, W. and Mittag, M. (2009). Analysis of flagellar phosphoproteins from Chlamydomonas reinhardtii. *Eukaryotic Cell* **8**, 922-932.

Buffone, M. G., Schindler, K. and Schultz, R. M. (2009). Overexpression of CDC14B causes mitotic arrest and inhibits zygotic genome activation in mouse preimplantation embryos. *Cell Cycle* **8**, 3904-3913.

Cao, Y., Park, A. and Sun, Z. (2010). Intraflagellar transport proteins are essential for cilia formation and for planar cell polarity. *J. Am. Soc. Nephrol.* **21**, 1326-1333.

Chen, J. N. and Fishman, M. C. (1996). Zebrafish tinman homolog demarcates the heart field and initiates myocardial differentiation. *Development* **122**, 3809-3816.

Cho, H. P., Liu, Y., Gomez, M., Dunlap, J., Tyers, M. and Wang, Y. (2005). The dual-specificity phosphatase CDC14B bundles and stabilizes microtubules. *Mol. Cell. Biol.* **25**, 4541-4551.

Clifford, D. M., Chen, C. T., Roberts, R. H., Feoktistova, A., Wolfe, B. A., Chen, J. S., McCollum, D. and Gould, K. L. (2008). The role of Cdc14 phosphatases in the control of cell division. *Biochem. Soc. Trans.* **36**, 436-438.

Cooper, M. S. and D'Amico, L. A. (1996). A cluster of noninvoluting endocytic cells at the margin of the zebrafish blastoderm marks the site of embryonic shield formation. *Dev. Biol.* **180**, 184-198.

Cueille, N., Salimova, E., Esteban, V., Blanco, M., Moreno, S., Bueno, A. and Simanis, V. (2001). Flp1, a fission yeast orthologue of the S. cerevisiae CDC14 gene, is not required for cyclin degradation or rum1p stabilisation at the end of mitosis. *J. Cell Sci.* **114**, 2649-2664.

Danos, M. C. and Yost, H. J. (1996). Role of notochord in specification of cardiac left-right orientation in zebrafish and Xenopus. *Dev. Biol.* **177**, 96-103.

Dawe, H. R., Farr, H. and Gull, K. (2007). Centriole/basal body morphogenesis and migration during ciliogenesis in animal cells. *J. Cell Sci.* **120**, 7-15.

Ernest, S., Rauch, G. J., Haffter, P., Geisler, R., Petit, C. and Nicolson, T. (2000). Mariner is defective in myosin VIIA: a zebrafish model for human hereditary deafness. *Hum. Mol. Genet.* **9**, 2189-2196.

Essner, J. J., Amack, J. D., Nyholm, M. K., Harris, E. B. and Yost, H. J. (2005). Kupffer's vesicle is a ciliated organ of asymmetry in the zebrafish embryo that initiates left-right development of the brain, heart and gut. *Development* **132**, 1247-1260.

Ferrante, M. I., Romio, L., Castro, S., Collins, J. E., Goulding, D. A., Stemple, D. L., Woolf, A. S. and Wilson, S. W. (2009). Convergent extension movements and ciliary function are mediated by ofd1, a zebrafish orthologue of the human oral-facial-digital type 1 syndrome gene. *Hum. Mol. Genet.* **18**, 289-303.

Gerdes, J. M., Davis, E. E. and Katsanis, N. (2009). The vertebrate primary cilium in development, homeostasis, and disease. *Cell* **137**, 32-45.

Gray, C. H., Good, V. M., Tonks, N. K. and Barford, D. (2003). The structure of the cell cycle protein Cdc14 reveals a proline-directed protein phosphatase. *EMBO J.* **22**, 3524-3535.

Haddon, C., Jiang, Y. J., Smithers, L. and Lewis, J. (1998). Delta-Notch signalling and the patterning of sensory cell differentiation in the zebrafish ear: evidence from the mind bomb mutant. *Development* **125**, 4637-4644.
Hans, S., Liu, D. and Westerfield, M. (2004). Pax8 and Pax2a function synergistically in otic specification, downstream of the Foxi1 and Dlx3b transcription factors. *Development* **131**, 5091-5102.
Higuchi, T. and Uhlmann, F. (2005). Stabilization of microtubule dynamics at anaphase onset promotes chromosome segregation. *Nature* **433**, 171-176.
Hurd, T., Zhou, W., Jenkins, P., Liu, C. J., Swaroop, A., Khanna, H., Martens, J., Hildebrandt, F. and Margolis, B. (2010). The retinitis pigmentosa protein RP2 interacts with polycystin 2 and regulates cilia-mediated vertebrate development. *Hum. Mol. Genet.* **19**, 4330-4344.
Kaiser, B. K., Zimmerman, Z. A., Charbonneau, H. and Jackson, P. K. (2002). Disruption of centrosome structure, chromosome segregation, and cytokinesis by misexpression of human Cdc14A phosphatase. *Mol. Biol. Cell* **13**, 2289-2300.
Kaiser, B. K., Nachury, M. V., Gardner, B. E. and Jackson, P. K. (2004). Xenopus Cdc14 alpha/beta are localized to the nucleolus and centrosome and are required for embryonic cell division. *BMC Cell Biol.* **5**, 27.
Kimmel, C. B. and Law, R. D. (1985). Cell lineage of zebrafish blastomeres. II. Formation of the yolk syncytial layer. *Dev. Biol.* **108**, 86-93.
Kimmel, C. B., Ballard, W. W., Kimmel, S. R., Ullmann, B. and Schilling, T. F. (1995). Stages of embryonic development of the zebrafish. *Dev. Dyn.* **203**, 253-310.
Ko, H. W., Norman, R. X., Tran, J., Fuller, K. P., Fukuda, M. and Eggenschwiler, J. T. (2010). Broad-minded links cell cycle-related kinase to cilia assembly and hedgehog signal transduction. *Dev. Cell* **18**, 237-247.
Kramer-Zucker, A. G., Olale, F., Haycraft, C. J., Yoder, B. K., Schier, A. F. and Drummond, I. A. (2005). Cilia-driven fluid flow in the zebrafish pronephros, brain and Kupffer's vesicle is required for normal organogenesis. *Development* **132**, 1907-1921.
Krasinska, L., de Bettignies, G., Fisher, D., Abrieu, A., Fesquet, D. and Morin, N. (2007). Regulation of multiple cell cycle events by Cdc14 homologues in vertebrates. *Exp. Cell Res.* **313**, 1225-1239.
Krauss, S., Johansen, T., Korzh, V. and Fjose, A. (1991). Expression of the zebrafish paired box gene pax[zf-b] during early neurogenesis. *Development* **113**, 1193-1206.
Kwon, H. J. and Riley, B. B. (2009). Mesendodermal signals required for otic induction: Bmp-antagonists cooperate with Fgf and can facilitate formation of ectopic otic tissue. *Dev. Dyn.* **238**, 1582-1594.
Liu, Q., Tan, G., Levenkova, N., Li, T., Pugh, E. N., Jr, Rux, J. J., Speicher, D. W. and Pierce, E. A. (2007a). The proteome of the mouse photoreceptor sensory cilium complex. *Mol. Cell. Proteomics* **6**, 1299-1317.
Liu, Y., Pathak, N., Kramer-Zucker, A. and Drummond, I. A. (2007b). Notch signaling controls the differentiation of transporting epithelia and multiciliated cells in the zebrafish pronephros. *Development* **134**, 1111-1122.
Long, S., Ahmad, N. and Rebagliati, M. (2003). The zebrafish nodal-related gene southpaw is required for visceral and diencephalic left-right asymmetry. *Development* **130**, 2303-2316.
Mailand, N., Lukas, C., Kaiser, B. K., Jackson, P. K., Bartek, J. and Lukas, J. (2002). Deregulated human Cdc14A phosphatase disrupts centrosome separation and chromosome segregation. *Nat. Cell Biol.* **4**, 317-322.
Marshall, W. F. and Rosenbaum, J. L. (2001). Intraflagellar transport balances continuous turnover of outer doublet microtubules: implications for flagellar length control. *J. Cell Biol.* **155**, 405-414.
Melby, A. E., Warga, R. M. and Kimmel, C. B. (1996). Specification of cell fates at the dorsal margin of the zebrafish gastrula. *Development* **122**, 2225-2237.
Milewski, W. M., Duguay, S. J., Chan, S. J. and Steiner, D. F. (1998). Conservation of PDX-1 structure, function, and expression in zebrafish. *Endocrinology* **139**, 1440-1449.
Mocciaro, A., Berdougo, E., Zeng, K., Black, E., Vagnarelli, P., Earnshaw, W., Gillespie, D., Jallepalli, P. and Schiebel, E. (2010). Vertebrate cells genetically deficient for Cdc14A or Cdc14B retain DNA damage checkpoint proficiency but are impaired in DNA repair. *J. Cell Biol.* **189**, 631-639.
Morgan, D. O. (1997). Cyclin-dependent kinases: engines, clocks, and microprocessors. *Annu. Rev. Cell Dev. Biol.* **13**, 261-291.
Munchberg, S. R., Ober, E. A. and Steinbeisser, H. (1999). Expression of the Ets transcription factors erm and pea3 in early zebrafish development. *Mech. Dev.* **88**, 233-236.
Neugebauer, J. M., Amack, J. D., Peterson, A. G., Bisgrove, B. W. and Yost, H. J. (2009). FGF signalling during embryo development regulates cilia length in diverse epithelia. *Nature* **458**, 651-654.
Odenthal, J. and Nusslein-Volhard, C. (1998). fork head domain genes in zebrafish. *Dev. Genes Evol.* **208**, 245-258.
Omori, Y., Zhao, C., Saras, A., Mukhopadhyay, S., Kim, W., Furukawa, T., Sengupta, P., Veraksa, A. and Malicki, J. (2008). Elipsa is an early determinant of ciliogenesis that links the IFT particle to membrane-associated small GTPase Rab8. *Nat. Cell Biol.* **10**, 437-444.
Ostrowski, L. E., Blackburn, K., Radde, K. M., Moyer, M. B., Schlatzer, D. M., Moseley, A. and Boucher, R. C. (2002). A proteomic analysis of human cilia: identification of novel components. *Mol. Cell. Proteomics* **1**, 451-465.
Oteiza, P., Koppen, M., Concha, M. L. and Heisenberg, C. P. (2008). Origin and shaping of the laterality organ in zebrafish. *Development* **135**, 2807-2813.
Pazour, G. J., Agrin, N., Leszyk, J. and Witman, G. B. (2005). Proteomic analysis of a eukaryotic cilium. *J. Cell Biol.* **170**, 103-113.
Phillips, B. T., Bolding, K. and Riley, B. B. (2001). Zebrafish fgf3 and fgf8 encode redundant functions required for otic placode induction. *Dev. Biol.* **235**, 351-365.
Platt, C. (1993). Zebrafish inner ear sensory surfaces are similar to those in goldfish. *Hear. Res.* **65**, 133-140.
Pugacheva, E. N., Jablonski, S. A., Hartman, T. R., Henske, E. P. and Golemis, E. A. (2007). HEF1-dependent Aurora A activation induces disassembly of the primary cilium. *Cell* **129**, 1351-1363.
Raible, F. and Brand, M. (2001). Tight transcriptional control of the ETS domain factors Erm and Pea3 by Fgf signaling during early zebrafish development. *Mech. Dev.* **107**, 105-117.
Reifers, F., Bohli, H., Walsh, E. C., Crossley, P. H., Stainier, D. Y. and Brand, M. (1998). Fgf8 is mutated in zebrafish acerebellar (ace) mutants and is required for maintenance of midbrain-hindbrain boundary development and somitogenesis. *Development* **125**, 2381-2395.
Rodier, G., Coulombe, P., Tanguay, P. L., Boutonnet, C. and Meloche, S. (2008). Phosphorylation of Skp2 regulated by CDK2 and Cdc14B protects it from degradation by APC(Cdh1) in G1 phase. *EMBO J.* **27**, 679-691.
Roehl, H. and Nusslein-Volhard, C. (2001). Zebrafish pea3 and erm are general targets of FGF8 signaling. *Curr. Biol.* **11**, 503-507.
Saito, R. M., Perreault, A., Peach, B., Satterlee, J. S. and van den Heuvel, S. (2004). The CDC-14 phosphatase controls developmental cell-cycle arrest in C. elegans. *Nat. Cell Biol.* **6**, 777-783.
Sakaguchi, T., Kikuchi, Y., Kuroiwa, A., Takeda, H. and Stainier, D. Y. (2006). The yolk syncytial layer regulates myocardial migration by influencing extracellular matrix assembly in zebrafish. *Development* **133**, 4063-4072.
Schindler, K. and Schultz, R. M. (2009a). CDC14B acts through FZR1 (CDH1) to prevent meiotic maturation of mouse oocytes. *Biol. Reprod.* **80**, 795-803.
Schindler, K. and Schultz, R. M. (2009b). The CDC14A phosphatase regulates oocyte maturation in mouse. *Cell Cycle* **8**, 1090-1098.
Schulte-Merker, S., Hammerschmidt, M., Beuchle, D., Cho, K. W., De Robertis, E. M. and Nusslein-Volhard, C. (1994). Expression of zebrafish goosecoid and no tail gene products in wild-type and mutant no tail embryos. *Development* **120**, 843-852.
Sobkowicz, H. M., Slapnick, S. M. and August, B. K. (1995). The kinocilium of auditory hair cells and evidence for its morphogenetic role during the regeneration of stereocilia and cuticular plates. *J. Neurocytol.* **24**, 633-653.
Solnica-Krezel, L., Stemple, D. L., Mountcastle-Shah, E., Rangini, Z., Neuhauss, S. C., Malicki, J., Schier, A. F., Stainier, D. Y., Zwartkruis, F., Abdelilah, S. et al. (1996). Mutations affecting cell fates and cellular rearrangements during gastrulation in zebrafish. *Development* **123**, 67-80.
Stegmeier, F. and Amon, A. (2004). Closing mitosis: the functions of the Cdc14 phosphatase and its regulation. *Annu. Rev. Genet.* **38**, 203-232.
Sullivan-Brown, J., Schottenfeld, J., Okabe, N., Hostetter, C. L., Serluca, F. C., Thiberge, S. Y. and Burdine, R. D. (2008). Zebrafish mutations affecting cilia motility share similar cystic phenotypes and suggest a mechanism of cyst formation that differs from pkd2 morphants. *Dev. Biol.* **314**, 261-275.
Sun, Z., Amsterdam, A., Pazour, G. J., Cole, D. G., Miller, M. S. and Hopkins, N. (2004). A genetic screen in zebrafish identifies cilia genes as a principal cause of cystic kidney. *Development* **131**, 4085-4093.
Tam, L. W., Wilson, N. F. and Lefebvre, P. A. (2007). A CDK-related kinase regulates the length and assembly of flagella in Chlamydomonas. *J. Cell Biol.* **176**, 819-829.
Thisse, C. and Thisse, B. (2008). High-resolution in situ hybridization to whole-mount zebrafish embryos. *Nat. Protoc.* **3**, 59-69.
Trautmann, S., Wolfe, B. A., Jorgensen, P., Tyers, M., Gould, K. L. and McCollum, D. (2001). Fission yeast Clp1p phosphatase regulates G2/M transition and coordination of cytokinesis with cell cycle progression. *Curr. Biol.* **11**, 931-940.
Trinkle-Mulcahy, L. and Lamond, A. I. (2006). Mitotic phosphatases: no longer silent partners. *Curr. Opin. Cell Biol.* **18**, 623-631.
Tsujikawa, M. and Malicki, J. (2004). Intraflagellar transport genes are essential for differentiation and survival of vertebrate sensory neurons. *Neuron* **42**, 703-716.
Wang, W. and Brautigan, D. L. (2008). Phosphatase inhibitor 2 promotes acetylation of tubulin in the primary cilium of human retinal epithelial cells. *BMC Cell Biol.* **9**, 62.
Wessely, O. and Obara, T. (2008). Fish and frogs: models for vertebrate cilia signaling. *Front. Biosci.* **13**, 1866-1880.

Whitfield, T. T., Riley, B. B., Chiang, M. Y. and Phillips, B. (2002). Development of the zebrafish inner ear. *Dev. Dyn.* **223**, 427-458.
Wolfe, B. A., McDonald, W. H., Yates, J. R., 3rd and Gould, K. L. (2006). Phospho-regulation of the Cdc14/Clp1 phosphatase delays late mitotic events in S. pombe. *Dev. Cell* **11**, 423-430.
Woods, A., Sherwin, T., Sasse, R., MacRae, T. H., Baines, A. J. and Gull, K. (1989). Definition of individual components within the cytoskeleton of Trypanosoma brucei by a library of monoclonal antibodies. *J. Cell Sci.* **93**, 491-500.
Wu, J., Cho, H. P., Rhee, D. B., Johnson, D. K., Dunlap, J., Liu, Y. and Wang, Y. (2008). Cdc14B depletion leads to centriole amplification, and its overexpression prevents unscheduled centriole duplication. *J. Cell Biol.* **181**, 475-483.
Yelon, D., Horne, S. A. and Stainier, D. Y. (1999). Restricted expression of cardiac myosin genes reveals regulated aspects of heart tube assembly in zebrafish. *Dev. Biol.* **214**, 23-37.
Zhao, C. and Malicki, J. (2007). Genetic defects of pronephric cilia in zebrafish. *Mech. Dev.* **124**, 605-616.